

Supporting Information Section

**Impacts of oxo interactions within actinyl metal organic materials:
Highlight on thermal expansion behaviour**

Maurice K. Payne, Mikaela M. Pynch, Matthew M. Jubinsky, Madeline C. Basile, and Tori Z. Forbes

Synthetic details

CAUTION: Neptunium-237 is a highly radioactive alpha emitter and as such is considered a health risk. Research involving this isotope and Uranium-238 is restricted to specialized laboratories and handled under appropriate regulatory controls and safe working practices.

UMON crystals were synthesized according to a previously published procedure with yields of 95%+.¹ The ²³⁷-Np was reprocessed from previous experiments and the Np(V) and Np(VI) stock were prepared in HNO₃ or HCl solutions. All other reagents were used as received.

Np(V)O₂(C₄NO₄H₆): A 25 μL aliquot of 0.2 M iminodiacetic acid and 25 μL of 0.2 M piperazine were added to a 3 mL glass vial. After thorough mixing, 50 μL of the 50 mM NpO₂⁺ in 1 M HNO₃ was added and the resulting solution was layered with acetone in a 1:1 vol:vol ratio. The solution was allowed to evaporate for several weeks, resulting in the formation of green plates at the bottom of the vial.

(N₂C₄H₁₂)₂[Np(V)O₂Cl₄]Cl: The neptunyl tetrachloride complex was synthesized by adding 200 μL of 20 mM Np(V)O₂⁺ stock solution in 1 M HCl to a solution containing 100 μL of 0.2 M iminodiacetate, 100 μL of a 0.2 M piperazine solution, and of 400 μL of methanol. After 3 weeks of slow evaporation, large green crystalline blocks precipitated from the solution.

Similar reactions as described for Np(V)O₂(C₄NO₄H₆) and (N₂C₄H₁₂)₂[Np(V)O₂Cl₄]Cl were attempted with the Np(VI) stock solution, but no crystals were obtained from these reactions.

Additional reactions with pyridine as the base and acetone as the crystallization agent were also attempted. Again, no crystalline solids were observed in these trials.

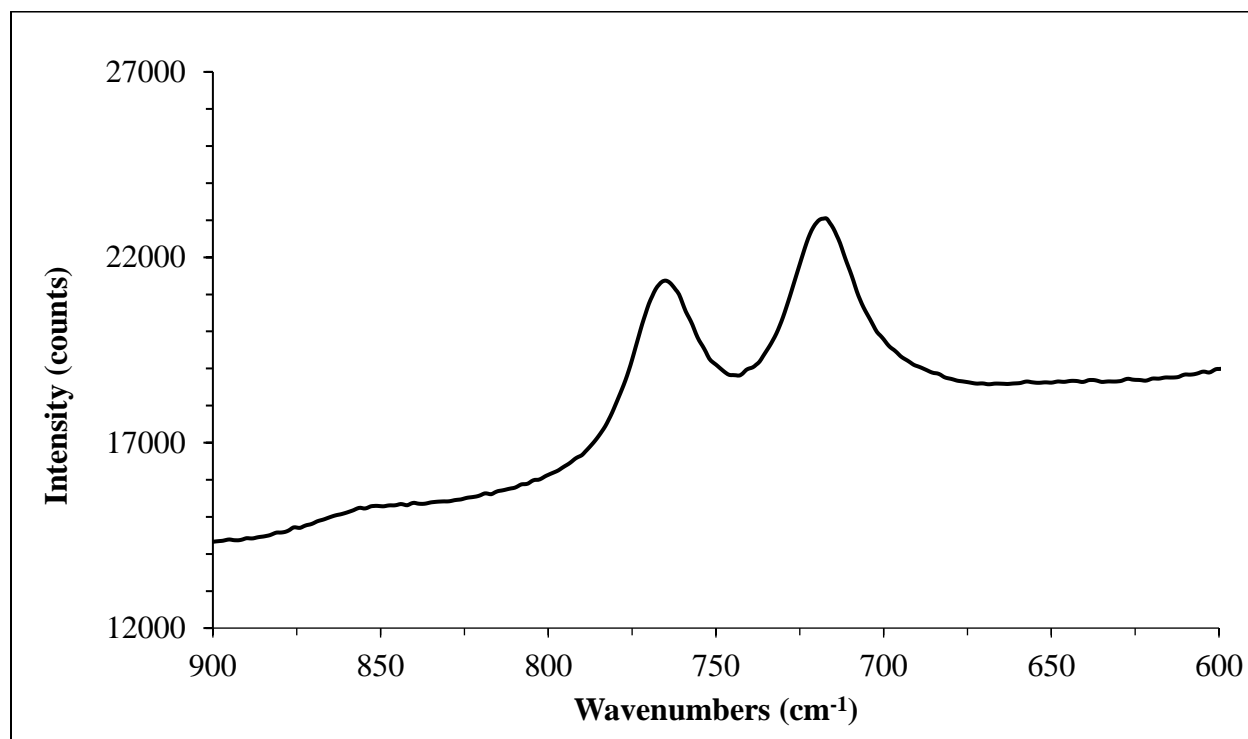


Figure S1. Raman spectra of the Np(V) stock in 1 M HNO₃ confirming the oxidation state with the symmetric stretch of the Np(V)O₂⁺ moiety present at 767 cm⁻¹. A second band associated with a nitrate stretch is located at 717 cm⁻¹.

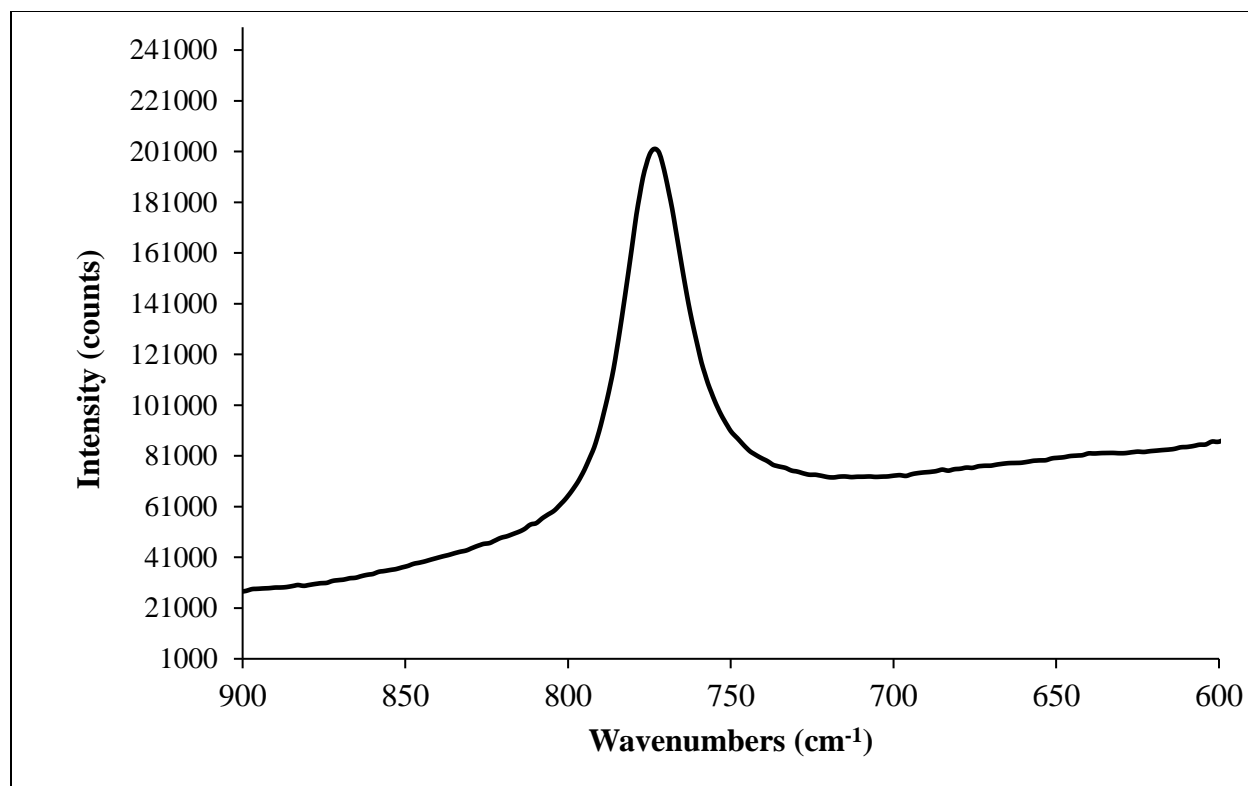


Figure S2. Raman spectra of the Np(V) stock in 1 M HCl with symmetric stretch of the Np(V)O_2^+ moiety present at 767 cm^{-1} .

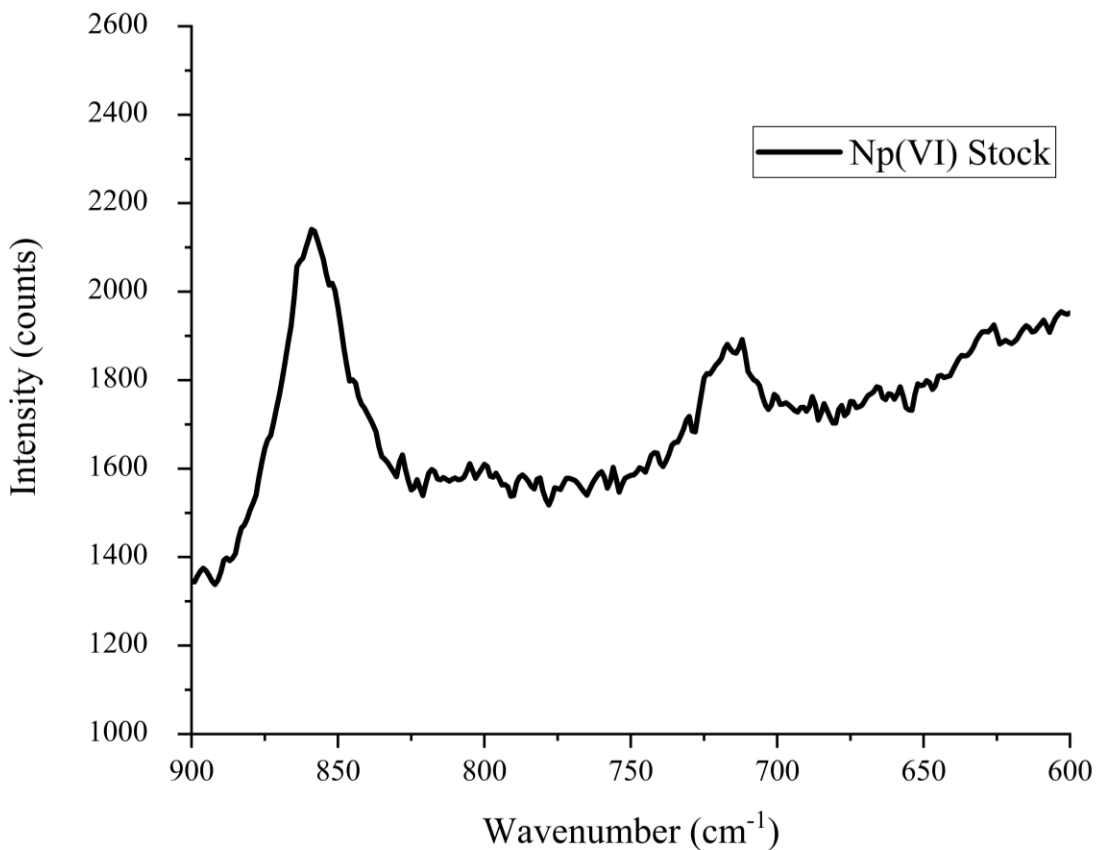


Figure S3. Raman Spectra of Np(VI) stock solution with the symmetric stretching band located at 852 cm^{-1} , corresponding to the $[\text{Np}(\text{VI})\text{O}_2]^{2+}$ species. A second band associated with a nitrate stretch is located at 717 cm^{-1} .

Structural characterization of initial materials at 100 K

Hydrated UMON samples and Np crystals were harvested directly from mother liquor and deposited into NVH immersion oil (MiTiGen) on a microscope slide. To obtain dehydrated samples, crystals of UMON were filtered (vacuum) and rinsed with acetone, followed by heating in an oven at 120° C for 24-56 h. We then placed the dehydrated crystals into immersion oil while still in the oven. Suitable single crystals of both hydration state were identified under optical microscopy and mounted on a cryoloop ($d = 50\text{ }\mu\text{m}$) and placed on the goniometer head once the cryostream temperature reached 100K.

Each sample was investigated with single crystal X-ray diffraction on a Bruker D8 Quest diffractometer equipped with a microfocus X-ray source (MoK α ; $\lambda = 0.71073 \text{ \AA}$) operating at 50kV and 1.0mA. We first did a fast scan (180° phi scan, $1.0^\circ/\text{frame}$) on each crystal to index and confirm hydration status, and followed that up with a full data collection to a resolution of at least 0.75 \AA . Data was collected with the Bruker APEX3² software package, and corrected the peak intensities for Lorentz, polarization and background effects. We used the program SADABS³ to perform an empirical absorption correction on each crystal. The structure was solved by intrinsic phasing methods and further refinement based on F^2 for all data was done using the SHELXT software⁴ (Version 5). Crystallographic information files (CIFs) for $\text{Np(V)O}_2(\text{C}_4\text{NO}_4\text{H}_6)$ and $(\text{N}_2\text{C}_4\text{H}_{12})_2[\text{Np(V)O}_2\text{Cl}_4]\text{Cl}$ can be obtained from the Cambridge Structural Database by quoting deposition numbers 1852343 and 1852341.

Table S1. Representative crystallographic parameters for the hydrated and dehydrated UMON sample at 100 K.

Compound	UMON Hydrated	UMON Dehydrated
Formula	$[(\text{UO}_2)(\text{C}_{10}\text{O}_8\text{N}_3\text{H}_{17})](\text{H}_2\text{O})_2$	$[(\text{UO}_2)(\text{C}_{10}\text{O}_8\text{N}_3\text{H}_{17})]$
FW (g/mol)	613.31	577.29
Space Group	$P\bar{3}$	$P\bar{3}$
a (Å)	22.228(3)	22.6865(8)
b (Å)	22.228(3)	22.6865(8)
c (Å)	6.6321(9)	6.5014(2)
α (°)	90	90
β (°)	90	90
γ (°)	120	120
V (Å ³)	2837.9(9)	2897.8(2)
Z	6	6
ρ (g/cm ³)	2.139	1.985
μ (mm ⁻¹)	8.642	8.450
F(000)	1716	1620
theta range	2.800-28.315	2.743-28.310
reflections	51220/4710	55232/4792
collected/unique	$R_{int} = 0.0433$	$R_{int} = 0.0471$
GOF on F ²	1.121	1.080
Final R indices (I > 2 σ)	$R_1 = 0.0225$ $wR_2 = 0.0587$	$R_1 = 0.0159$ $wR_2 = 0.0358$
R indices (all data)	$R_1 = 0.0260$ $wR_2 = 0.0604$	$R_1 = 0.0189$ $wR_2 = 0.0368$
Largest peak/hole (Å ⁻³)	4.115, -1.302	2.268, -1.261

Table S2. Selected crystallographic parameters for $\text{Np(V)O}_2(\text{C}_4\text{NO}_4\text{H}_6)$ and $(\text{N}_2\text{C}_4\text{H}_{12})_2[\text{Np(V)O}_2\text{Cl}_4]\text{Cl}$.

Compound	$\text{Np(V)O}_2(\text{C}_4\text{NO}_4\text{H}_6)$	$(\text{N}_2\text{C}_4\text{H}_{12})_2[\text{Np(V)O}_2\text{Cl}_4]\text{Cl}$
FW (g/mol)	401.10	622.56
Space Group	<i>Pmmn</i>	<i>P-1</i>
a (Å)	8.2246(8)	7.4041(10)
b (Å)	9.7709(8)	10.4454(11)
c (Å)	4.5380(4)	12.3566(16)
α (°)	90	76.494(10)
β (°)	90	89.313(9)
γ (°)	90	71.795(7)
V (Å ³)	364.68(6)	880.8(2)
Z	2	2
ρ (g/cm ³)	3.653	2.347
μ (mm ⁻¹)	14.239	6.662
F(000)	356	588
theta range	3.238 to 33.248	2.115 to 27.975
Limiting indices	-12<h<12 -15<k<15 -6<l<6	-9<h<9 -13<k<13 -16<l<16
reflections	21137 / 772	55386 / 4219
collected/unique	$R_{\text{int}} = 0.0421$	$R_{\text{int}} = 0.0350$
GOF on F ²	1.297	1.324
Final R indices ($I > 2\sigma$)	$R_1 = 0.0187$ $wR_2 = 0.0466$	$R_1 = 0.0102$ $wR_2 = 0.0250$
R indices (all data)	$R_1 = 0.0193$ $wR_2 = 0.0467$	$R_1 = 0.0103$ $wR_2 = 0.0408$
Largest peak/hole (Å ⁻³)	3.682, -2.614	0.469, -1.738

Table S3. Selected bond distances for $\text{Np(V)O}_2(\text{C}_4\text{NO}_4\text{H}_6)$.

Np(1)-O(1')	1.821(4)	O(1)-C(1)	1.265(6)
Np(1)-O(1') ^a	1.821(4)	N(1)-C(2) ^d	1.474(6)
Np(1)-O(2)	2.506(4)	N(1)-C(2)	1.474(6)
Np(1)-O(2) ^a	2.506(4)	C(1)-O(2)	1.257(7)
Np(1)-O(1) ^b	2.538(4)	C(1)-C(2)	1.487(7)
Np(1)-O(1) ^c	2.538(4)		
Np(1)-O(1) ^a	2.686(4)		
Np(1)-O(1)	2.686(4)		

a: $-x+3/2, -y+1/2, z$; b: $-x+3/2, -y+1/2, z-1$; c: $x, y, z-1$; d: $-x+3/2, -y+3/2, z$.

Table S4. Selected bond distances for $(\text{N}_2\text{C}_4\text{H}_{12})_2[\text{Np}(\text{V})\text{O}_2\text{Cl}_4]\text{Cl}$.

Np(1)-O(1)	1.830(2)
Np(1)-O(2)	1.856(2)
Np(1)-C1(1)	2.7369(7)
Np(1)-C1(2)	2.7384(6)
Np(1)-C1(3)	2.7645(7)
Np(1)-C1(4)	2.7772(6)

Variable Temperature Single Crystal X-Ray Diffraction of UMON

We replicated this procedure (fast scan, then full data collection and workup) at each temperature of interest from 100K to 260K specifically focusing in the 200-260K range in 10K steps. A Cryostream 800 cold head (Oxford Cryosystems) with nitrogen gas flow modulated the sample temperature and the temperature was held for 15 min so the sample could equilibrate before beginning data collection. The exposure time was also increased throughout the temperature experiment so that each data collection resulted in roughly the same intensity of reflections. We undertook this overall scheme for three different UMON crystals, from three different synthetic batches for both the hydrated and dehydrated nanotubes for a total of 48 individual data sets. The structures were determined using the protocol described *vide supra*.

Table S5. Representative structural parameters for UMON sample collected between 200-260 K.

Temperature	200 K dehydrated	230 K dehydrated	260 K dehydrated	200 K hydrated	230 K hydrated	260 K hydrated
a (Å)	22.707(4)	22.667(4)	22.6680(6)	22.4104(7)	22.448(5)	22.455(6)
c (Å)	6.5152(8)	6.5143(8)	6.5169(2)	6.6056(2)	6.5723(10)	6.5551(13)
V (Å ³)	2909.2(10)	2898.6(11)	2900.00(18)	2873.0(2)	2868.2(13)	2862.6(16)
F(000)	1620	1620	1620	1716	1716	1716
theta range	2.74 – 28.326	2.745-28.375	2.745-28.375	2.099 – 28.703	2.772 -28.376	2.771 - 28.371
reflections collected/unique	55839/4638 R _{int} = 0.0509	55673/4828 R _{int} = 0.0521	55357/4808 R _{int} = 0.0580	44088/4963 R _{int} = 0.0497	41169 / 4780 R _{int} = 0.0475	41101 / 4780 R _{int} = 0.0528
GOF on F ²	1.144	1.055	1.053	1.114	1.072	1.072
Final R indices (I > 2σ)	R ₁ = 0.0195 wR ₂ = 0.0504	R ₁ = 0.0223 wR ₂ = 0.0559	R ₁ = 0.0342 wR ₂ = 0.0882	R ₁ = 0.0300 wR ₂ = 0.0741	R ₁ = 0.0287 wR ₂ = 0.0772	R ₁ = 0.0381 wR ₂ = 0.1022
R indices (all data)	R ₁ = 0.0243 wR ₂ = 0.0523	R ₁ = 0.0281 wR ₂ = 0.0556	R ₁ = 0.0429 wR ₂ = 0.0938	R ₁ = 0.0377 wR ₂ = 0.0781	R ₁ = 0.0352 wR ₂ = 0.0808	R ₁ = 0.0477 wR ₂ = 0.1088

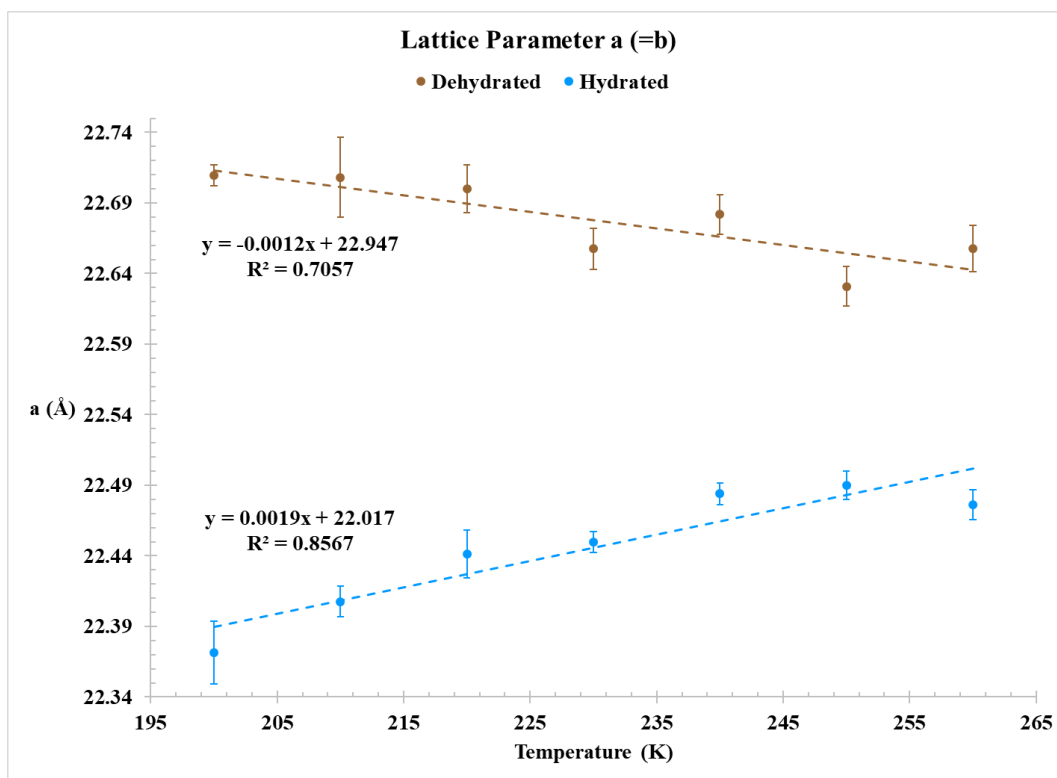


Figure S4. Changes in the a parameter as a function of temperature for hydrated and dehydrated UMON. Data points are the average of three experiments, and error bars represent the standard error.

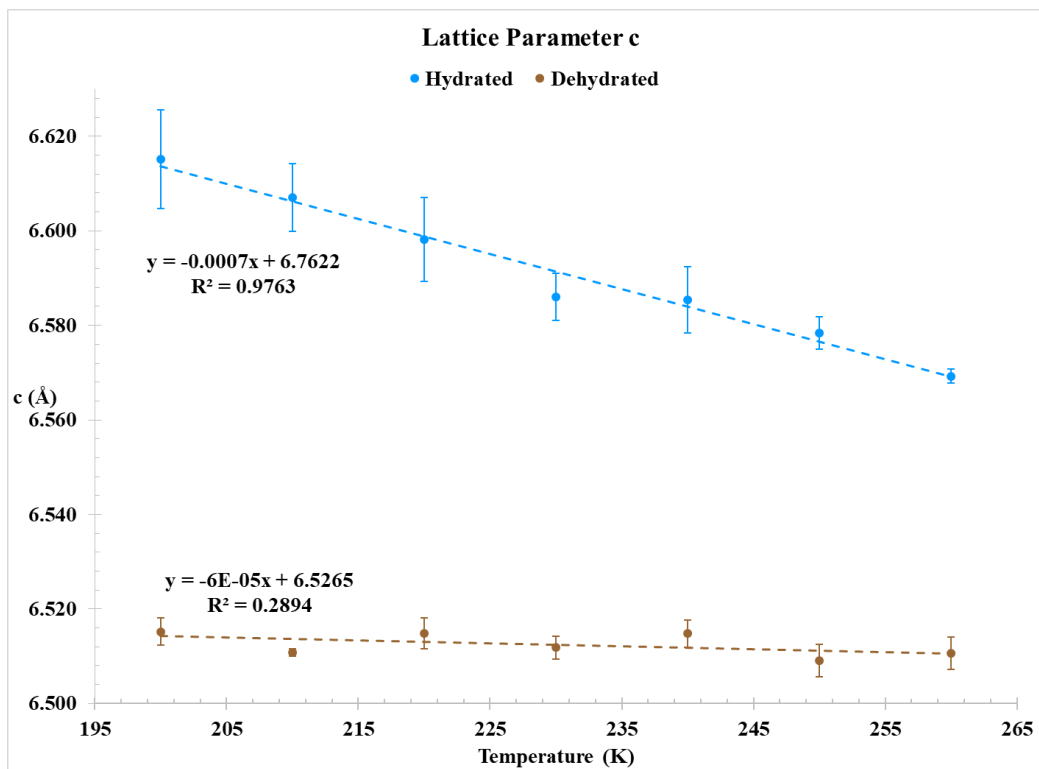


Figure S5. Variations in the c parameter as a function of temperature for hydrated and dehydrated UMON. Data points are the average of three experiments, and error bars represent the standard error.

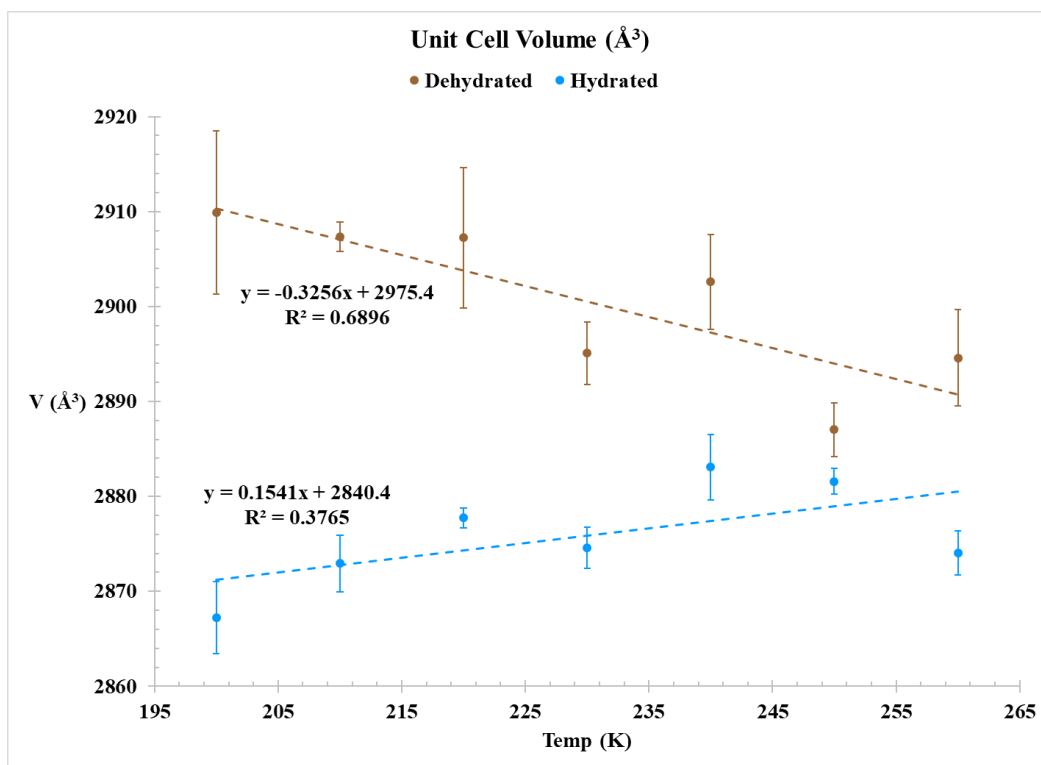


Figure S6. Changes in the cell volume as a function of temperature for hydrated and dehydrated UMON. Data points are the average of three experiments, and error bars represent the standard error.

Structural images

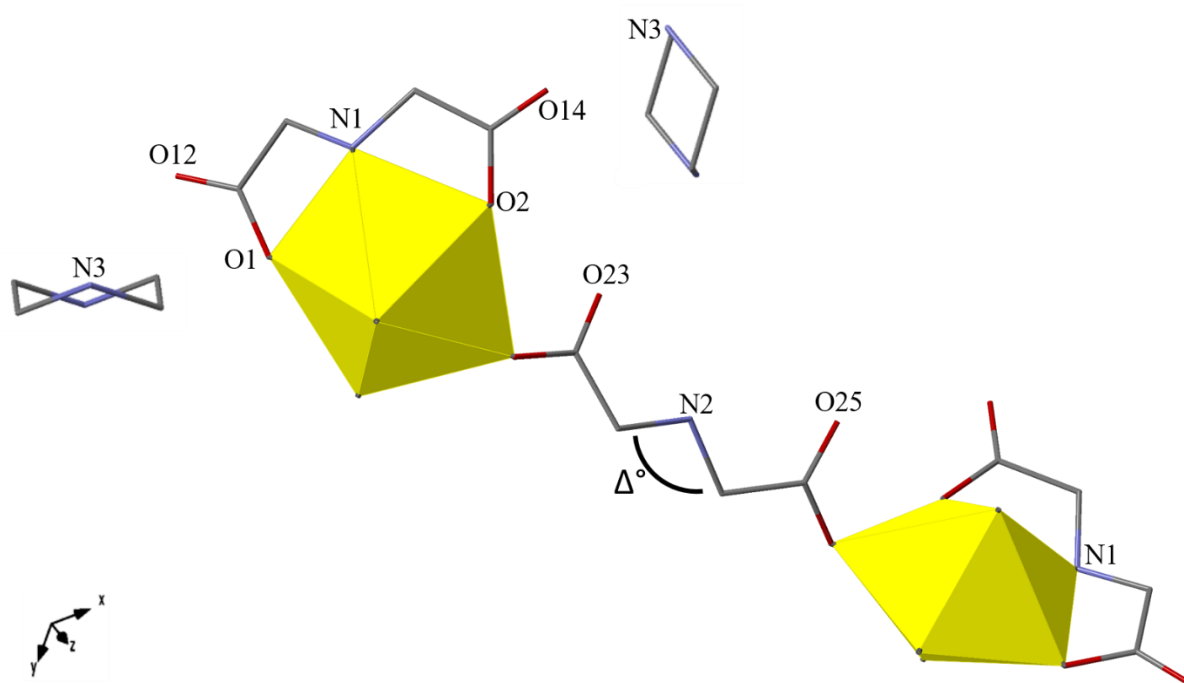


Figure S7. C–N–C bond angle within the iminodiacetate linker for UMON that varies with heating (200–260K = $\sim -0.5^\circ$). The canted angle of the ligand leads to isotropic negative thermal behaviour within the UMON material. U atoms are depicted as yellow polyhedra and the iminodiacetate and lattice piperazinium molecules are illustrated as wire representations. H atoms are removed for clarity. Select hydrogen bonding atoms are labeled and highlighted in table below.

D--A	Representative Distance, Å (from 200K dehydrated data)
N3--O12	2.784(3)
N3--O25 ^a	2.790(3)
N3--O14 ^b	2.857(4)
N2--O1 ^c	2.840(3)
N2--O2 ^d	2.930(3)
N1--O23 ^e	3.286(4)

a: $x-y, x, -z+1$ *b:* $x-y, x, -z$ *c:* $y, -x+y, -z+1$ *d:* $x, y, z+1$ *e:* $x, y, z-1$

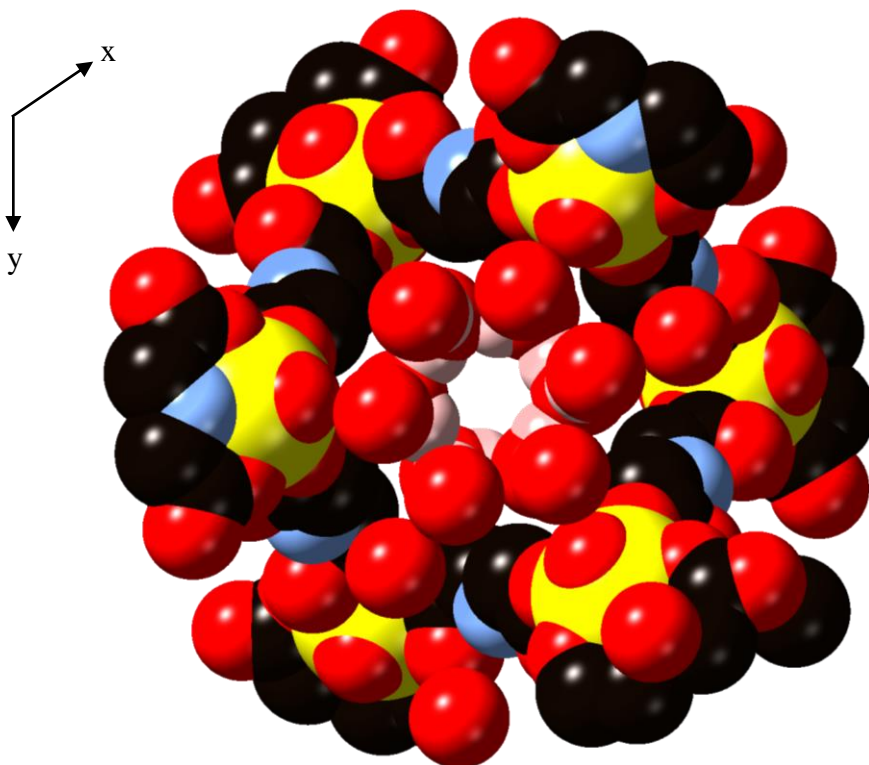


Figure S8. Space filling model of a single UMON nanotube structure with sphere size representative of the van der Waals radii for each element. The U, O, C, N, and H atoms are depicted as yellow, red, black, light blue, and pink spheres, respectively.

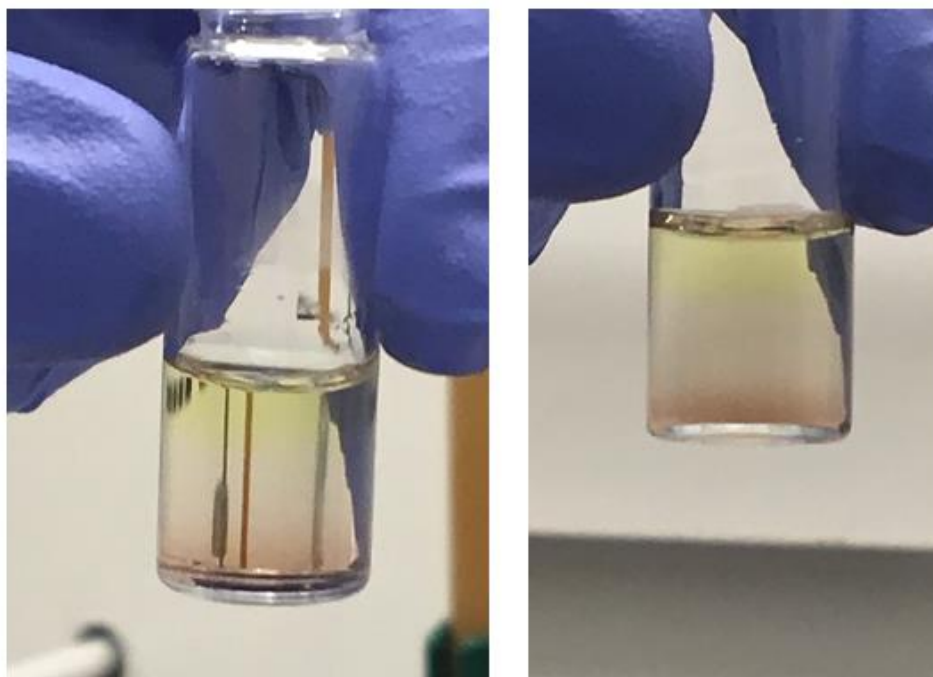


Figure S9. Images depicting the reduction of Np(VI) to Np(V) upon addition of pyridine. The first picture was taken after the addition of pyridine and the second image was taken two minutes later.

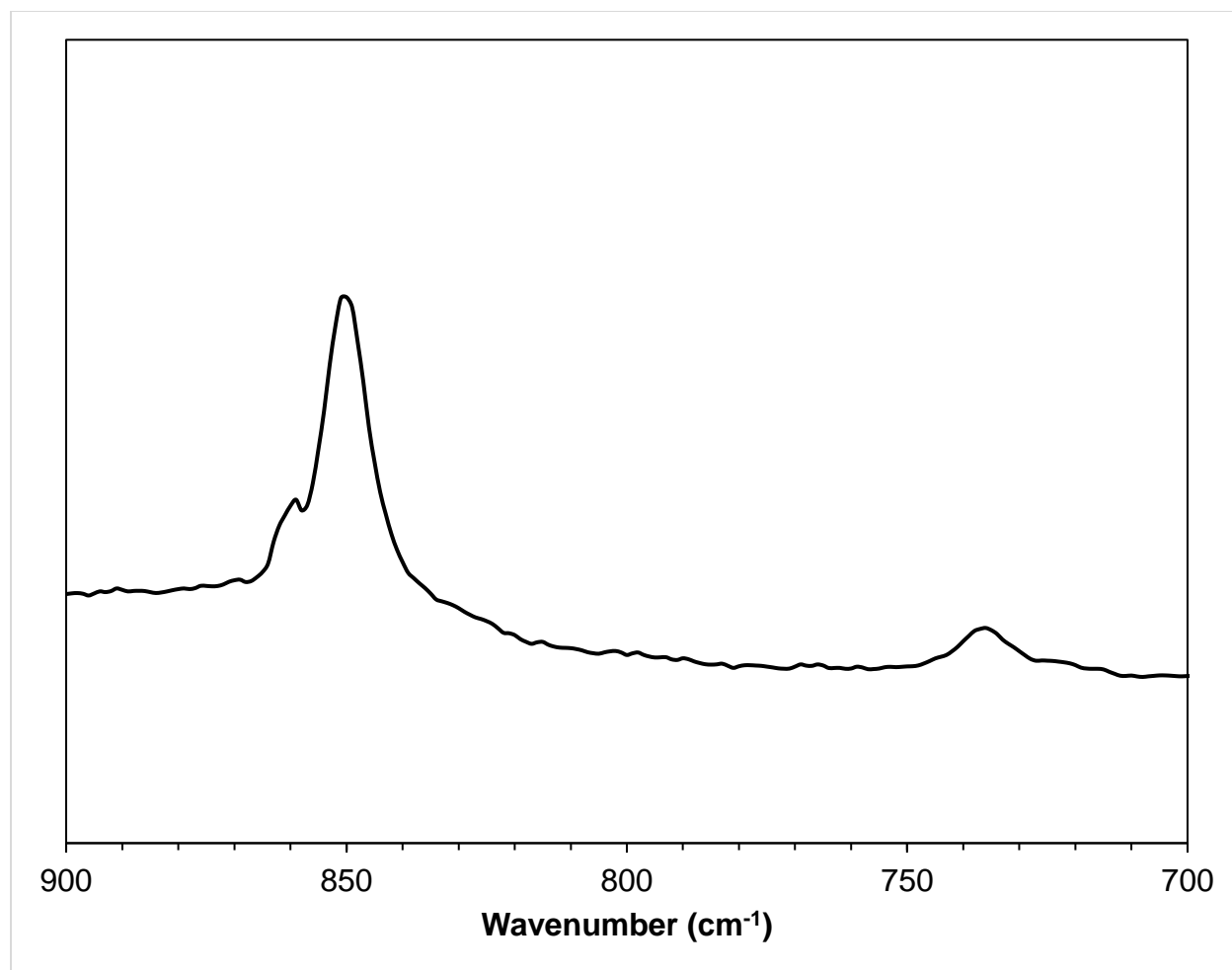


Figure S10. Raman spectra of the initial Np(VI) in 1 M HNO₃:iminodiacetate:piperazine (1:2:3 molar ratio) solution with a cosolvent of methanol. The band at 852 cm⁻¹ corresponds to the Np(VI)O₂²⁺ symmetric stretch (ν_1). There is ingrowth of the NpO₂⁺ symmetric stretching band at 740 cm⁻¹, which is likely due to reduction of the Np(VI) stock solution to form Np(V) in solution.

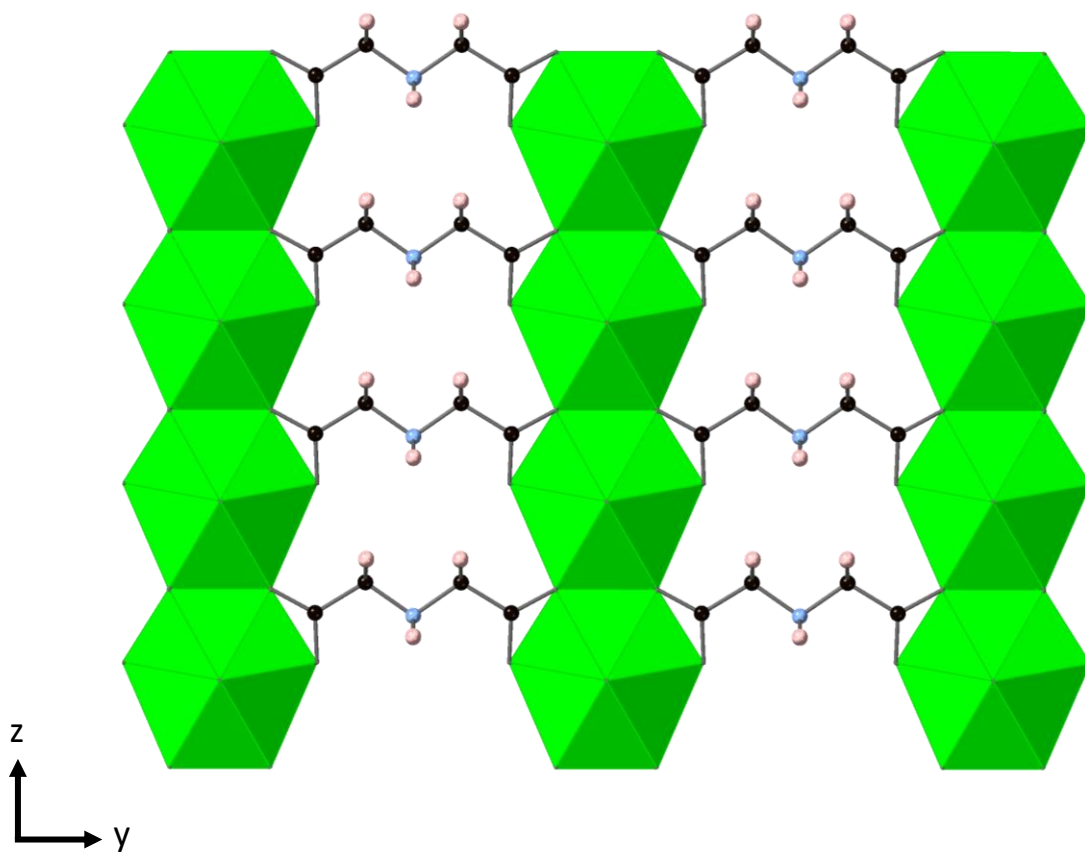


Figure S11. Extended sheet topology observed in $\text{Np}(\text{V})\text{O}_2(\text{C}_4\text{NO}_4\text{H}_6)$. The Np is depicted as green polyhedral and the C, N, and H atoms are represented by black, light blue, and pink spheres, respectively. The O atoms have been removed from the image for clarity.

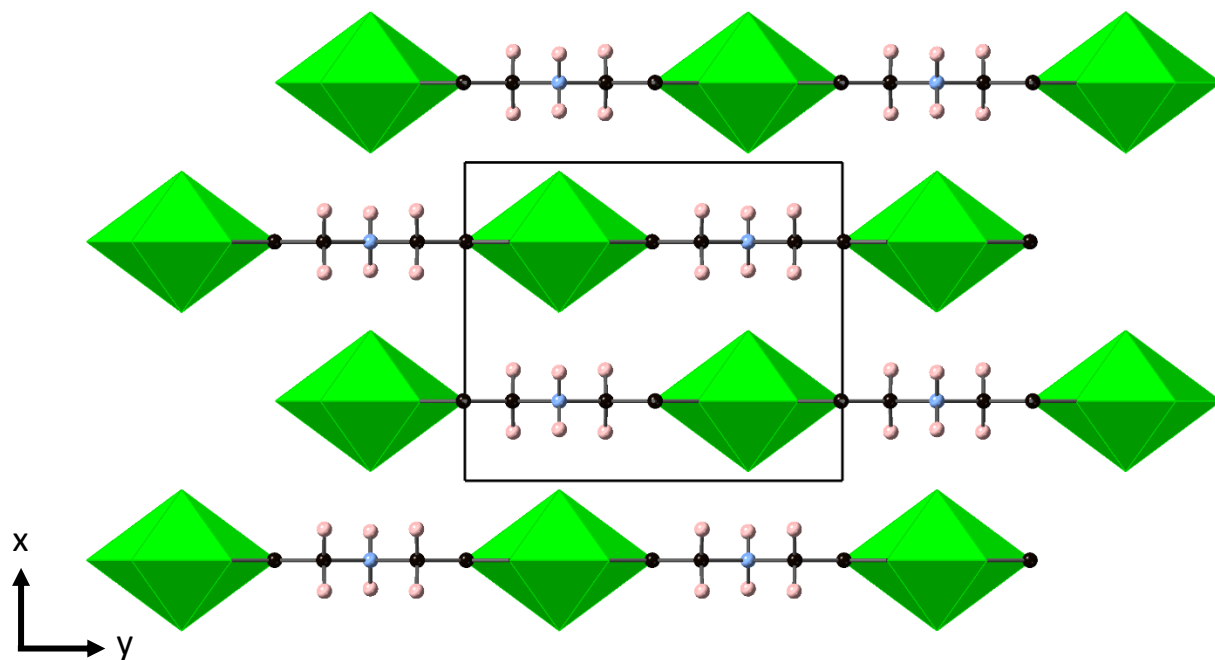


Figure S12. Extended three-dimensional lattice for $\text{Np(V)O}_2(\text{C}_4\text{NO}_4\text{H}_6)$ with Np represented by green polyhedra, whereas the C, N, and H atoms are depicted as by black, light blue, and pink spheres, respectively. The O atoms have been removed from the image for clarity.

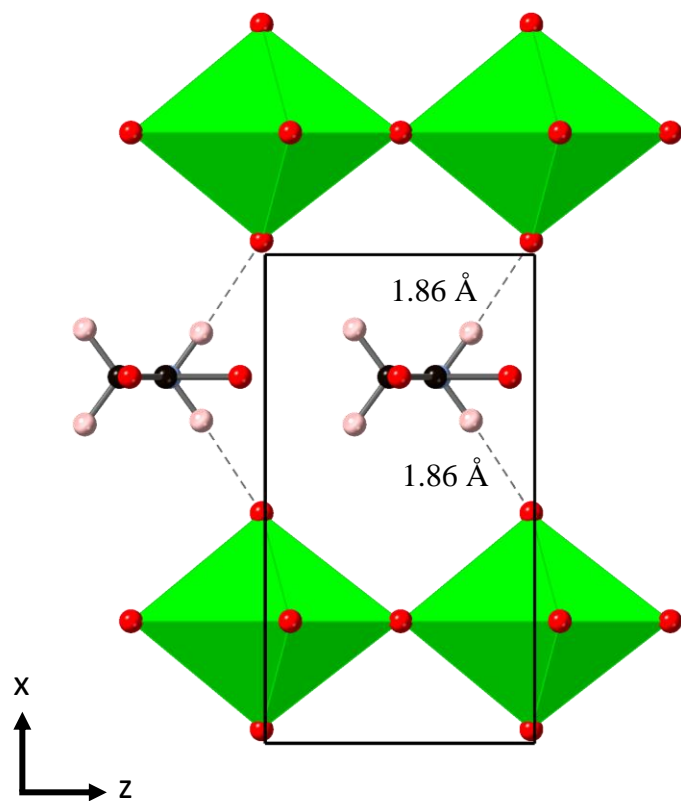


Figure S13. Hydrogen bonding within the $\text{Np(V)O}_2(\text{C}_4\text{NO}_4\text{H}_6)$ compound is depicted as dashed lines. The hydrogen to acceptor (Np=O) distances are 1.86 \AA . Np represented by green polyhedra, whereas the O, C, N, and H atoms are depicted as red, black, light blue, and pink spheres.

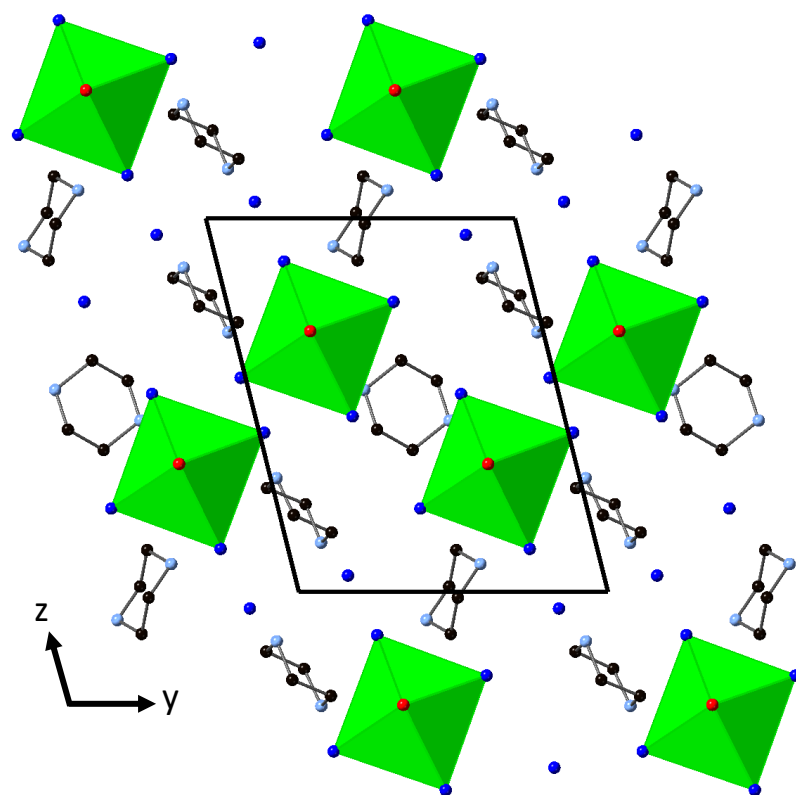


Figure S14. Extended lattice for $(\text{N}_2\text{C}_4\text{H}_{12})_2[\text{Np}(\text{V})\text{O}_2\text{Cl}_4]\text{Cl}$ shown down the a axis. The Np is represented with green polyhedra and the O, Cl, C, and N atoms are depicted with red, blue, black, and light blue spheres, respectively. H atoms have been removed for clarity.

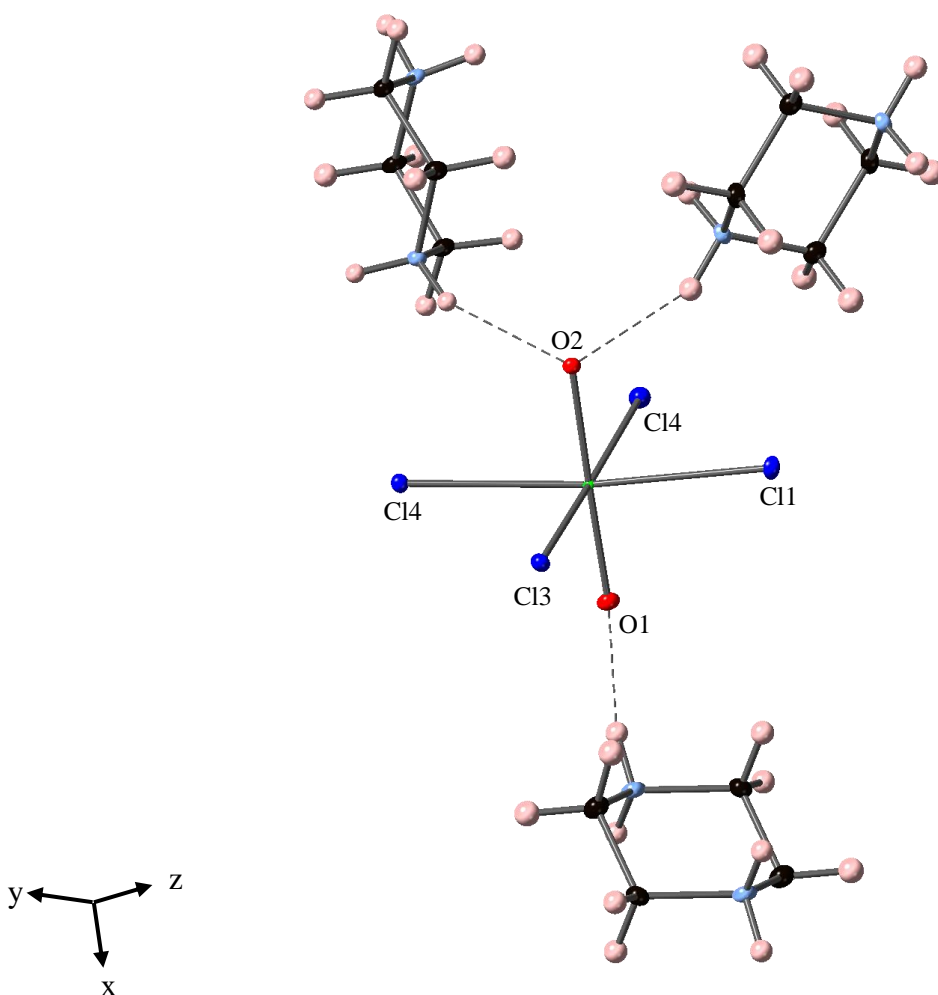


Figure S15. Hydrogen bonding occurs between the neptunyl oxo groups and the amine groups on the piperazinium cation for $(N_2C_4H_{12})_2[Np(V)O_2Cl_4]Cl$. The hydrogen to acceptor distance for O1 is 1.88 Å and O2 engages in a bifurcated bond with distances of 2.03 and 2.13 Å. Np, O, Cl, C, and N atoms are illustrated with green, red, blue, black, light blue, and pink ellipsoids, respectively.

Variable Temperature Single Crystal X-Ray Diffraction of $(N_2C_4H_{12})_2[Np(V)O_2Cl_4]Cl$

Utilizing the earlier described procedure for variable temperature experiments of UMON crystals (fast scan, then full data collection of omega and phi scans) for the Np(V) crystal, we executed collections at each temperature of interest (100K, 200-260K in 10K steps, and 298K). A Cryostream 800 cold head (Oxford Cryosystems) with nitrogen gas flow modulated the sample

temperature and the temperature was held for 900 seconds allowing the target temperature to be achieved before beginning data collections. Full crystallographic analysis (unit cell determination, integration, scaling, space group determination, structure solution) was performed for all 10 individual data sets to allow for accurate cell parameters and confirmation of atomic positions. Reported bond lengths and distances are those associated with the 100K data collection.

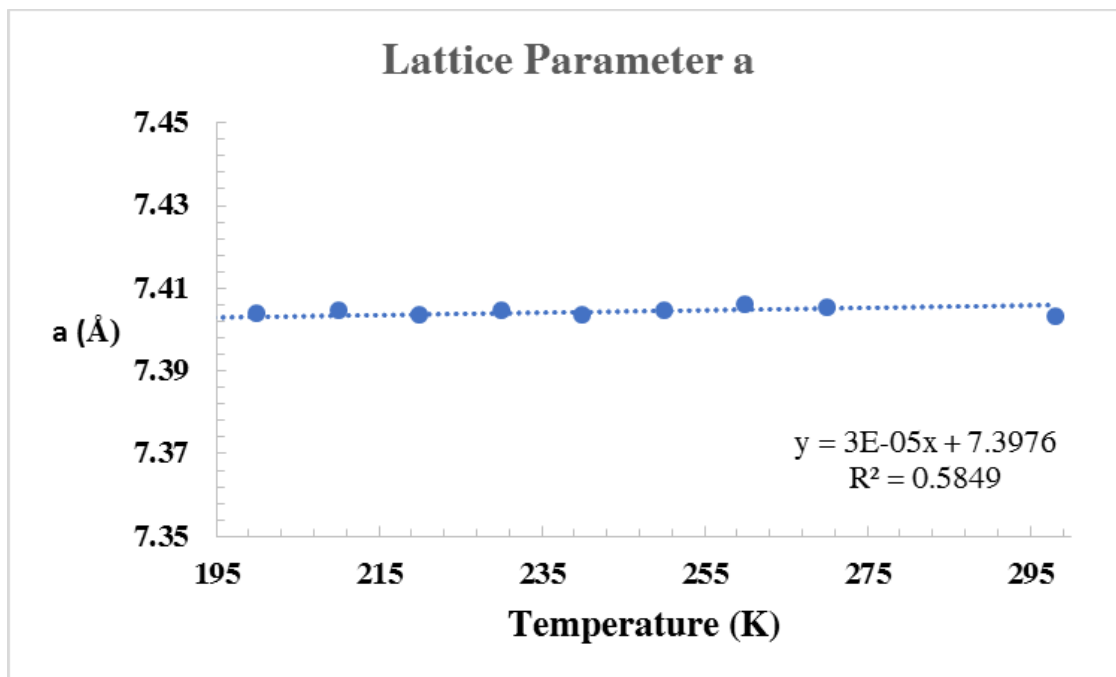


Figure S16. Changes in the a parameter as a function of temperature for $(N_2C_4H_{12})_2[Np(V)O_2Cl_4]Cl$.

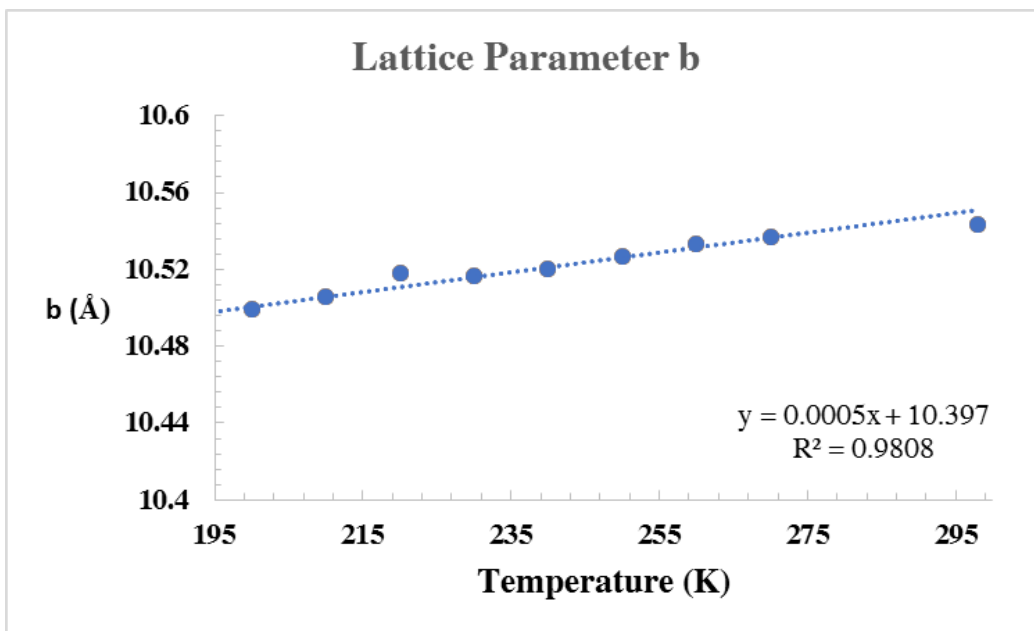


Figure S17. Variations in the b parameter as a function of temperature for $(\text{N}_2\text{C}_4\text{H}_{12})_2[\text{Np}(\text{V})\text{O}_2\text{Cl}_4]\text{Cl}$.

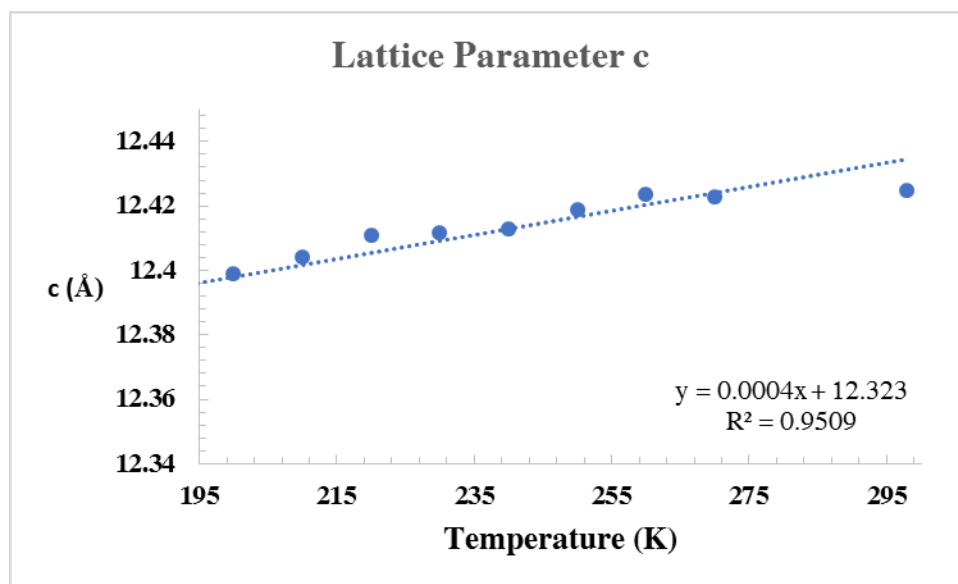


Figure S18. Variations in the c parameter as a function of temperature for $(\text{N}_2\text{C}_4\text{H}_{12})_2[\text{Np}(\text{V})\text{O}_2\text{Cl}_4]\text{Cl}$.

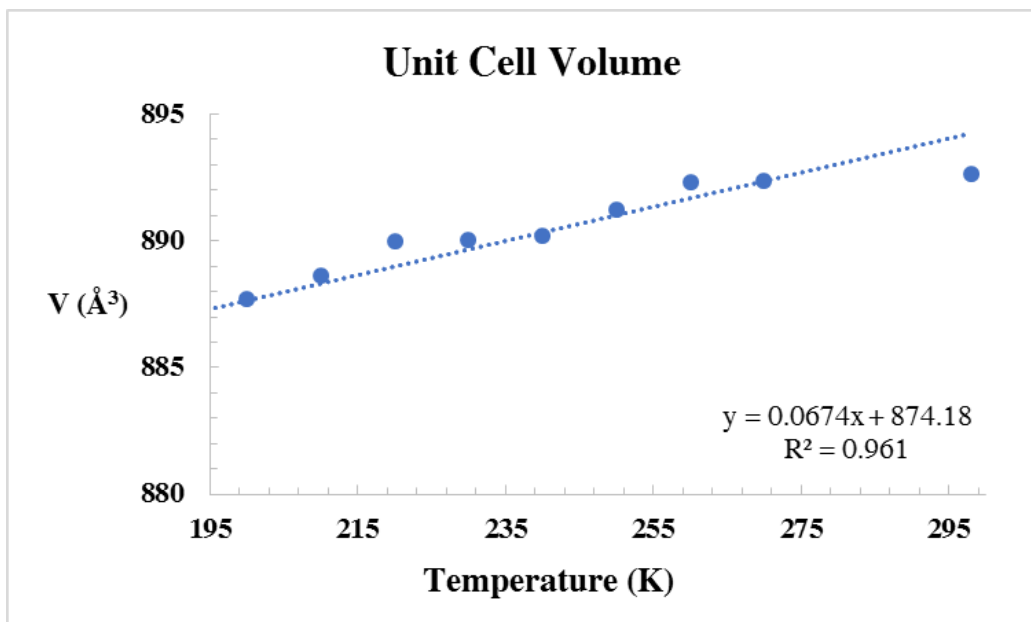


Figure S19. Changes in the cell volume as a function of temperature for $(\text{N}_2\text{C}_4\text{H}_{12})_2[\text{Np}(\text{V})\text{O}_2\text{Cl}_4]\text{Cl}$.

Table S5. Representative structural parameters for (N₂C₄H₁₂)₂[Np(V)O₂Cl₄]Cl collected between 200-260 K.

Temperature	200 K	230 K	260 K
a (Å)	7.4040(4)	7.4048(4)	7.4062(5)
b (Å)	10.4994(5)	10.5168(5)	10.5336(6)
c (Å)	12.3991(6)	12.4117(6)	12.4237(8)
α (°)	76.520(2)	76.509(2)	76.510(2)
β (°)	89.217(2)	89.181(2)	89.155(2)
γ (°)	71.634(2)	71.605(2)	71.570(2)
V (Å ³)	887.71(8)	890.02(8)	892.31(10)
F(000)	588	588	584
theta range	1.692 - 27.103	1.691 - 27.243	1.689 - 27.211
reflections	51059 / 3926	51528 / 3987	50924 / 3987
collected/unique	R _{int} = 0.0304	R _{int} = 0.0295	R _{int} = 0.0298
GOF on F ²	1.153	1.165	1.078
Final R indices (I > 2σ)	R ₁ = 0.0133 wR ₂ = 0.0336	R ₁ = 0.0128 wR ₂ = 0.0320	R ₁ = 0.0138 wR ₂ = 0.0495
R indices (all data)	R ₁ = 0.0135 wR ₂ = 0.0381	R ₁ = 0.0131 wR ₂ = 0.0321	R ₁ = 0.0142 wR ₂ = 0.0247

Table S6. Principle coefficients of the thermal expansion for (N₂C₄H₁₂)₂[Np(V)O₂Cl₄]Cl and corresponding approximate crystallographic direction calculated with PASCAL.

Axis	α (MK ⁻¹)	Crystallographic direction
X ₁	-2.8(9)	1 0 0
X ₂	+30(3)	0 0 1
X ₃	+49(3)	0 1 0
V	+80(5)	

References

1. D. K. Unruh, K. Gojdas, A. Libo and T. Z. Forbes, *J. Am. Chem. Soc.*, 2013, **135**, 7398-1401.
2. G. M. Sheldrick, *APEX3*, 2015.
3. G. M. Sheldrick, *SADABS*, 1996.
4. G. M. Sheldrick, *Acta Crystallographica Section A: Foundations of Crystallography*, 2008, **64**, 112-122.